Macromolecules

ARTICLE

pubs.acs.org/Macromolecules

Controlling Domain Orientations in Thin Films of AB and ABA Block Copolymers

Thai Vu,[†] Nikhila Mahadevapuram,[†] Ginusha M. Perera, and Gila E. Stein*

Department of Chemical and Biomolecular Engineering, University of Houston, Houston, Texas 77204-4004, United States

ABSTRACT: Domain orientations in thin films of lamellar copolymers are evaluated as a function of copolymer architecture, film thickness, and processing conditions. Two copolymer architectures are considered: An AB diblock of poly(styrene-*b*-methyl methacrylate) and an ABA triblock of poly(methyl methacrylate-*b*-styrene-*b*-methyl methacrylate). All films are cast on substrates that are energetically neutral with respect to the copolymer constituents. Film structures are evaluated with optical microscopy, atomic force microscopy, and grazing-incidence small-angle X-ray scattering. For AB diblock copolymers, the domain orientations are very sensitive to film thickness, annealing temperature, and imperfections in the "neutral" substrate coating: Diblock domains are oriented perpendicular to the substrate when annealing temperature is elevated (≥220 °C) and defects in the substrate coating are minimized; otherwise, parallel or mixed parallel/perpendicular domain orientations are detected for most film thicknesses. For ABA triblock copolymers, the perpendicular domain orientation is stable for all the film thicknesses and processing conditions that were studied. The orientations of diblock and triblock copolymers are consistent with recent works that consider architectural effects when calculating the copolymer surface tension (Macromolecules 2006, 39, 9346 and Macromolecules 2010, 43, 1671). Significantly, the data demonstrate that triblocks are easier to process for applications in nanopatterning—in particular, when high-aspect-ratio nanostructures are required. However, both diblock and triblock films contain a high density of "tilted" or bent domains, and these kinetically trapped defects should be minimized for most patterning applications.

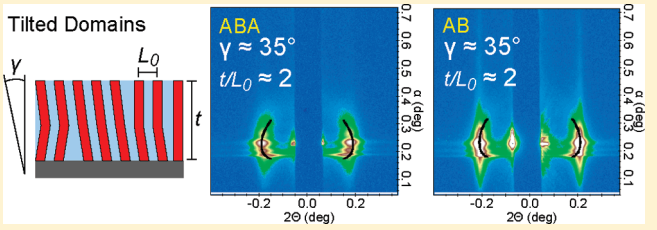

INTRODUCTION

Thin films of block copolymers are attractive as low-cost templates for nanopatterning.[1−3] Applications in semiconductor manufacturing will require control over the size and shape, position, and orientation of copolymer domains.[2,3] Domain sizes and shapes are determined by copolymer molecular weight and composition,[4] respectively, while positions can be controlled with epitaxial or topographical templates.[5−8] Domain orientations are largely determined by surface energetics and confinement effects, and these factors are most thoroughly studied for diblock (AB) copolymers.[3,9] The objective of our current work is to identify the factors that control domain orientations in thin films of triblock (ABA) copolymers.

For most applications in nanopattering, a thin copolymer film is prepared by spin-casting on a substrate, so domains are confined between a hard surface and a "soft" air interface. Typically, each interface favors wetting by one of the blocks, and this preference drives a layering of the domains parallel to the substrate.[9,10] For example, consider a thin film of lamellar poly(styrene-*b*-methyl methacrylate) (PS−PMMA) on a silicon substrate: PS has a slightly lower surface energy than PMMA, while PMMA is strongly preferred over PS at the substrate.[11,12] These asymmetric boundary conditions favor a parallel domain orientation that persists through the film thickness.[13−15] In these asymmetric systems, film thickness is commensurate with the equilibrium domain size when $t = (n + {}^1/_2)L_0$, where L_0 is the domain periodicity and n is an integer. When film thickness is incommensurate with L_0, entropic frustration drives the formation of islands or holes at the free surface.[12,15] The film then consists of regions with two distinct thicknesses that are both commensurate with L_0.[10]

Domains that are oriented parallel to the substrate are not useful for nanopatterning, so a variety of methods have been developed to produce the desired perpendicular orientation.[2,3] Examples include application of an electric field,[16] rough substrates,[17,18] directional solvent evaporation,[19,20] adding surfactants or surface-active nanoparticles,[21−23] blending with homopolymer,[24] and preparing "neutral" substrates by tuning the polymer−substrate interfacial energy.[25−27] The latter approach is very popular because the technique can be applied to many copolymer systems and is easy to integrate with standard manufacturing protocols.[3] However, perpendicular domains are only stable on neutral substrates through a limited range of film thickness.[28−33] The film thickness constraint is understood by considering the interfacial energetics that control domain orientations: Perpendicular orientations incur a gain in surface energy. If the copolymer is comprised of segments with similar surface energies, such as PS and PMMA, then this additional enthalpic contribution can be offset by other factors. For example, when film thickness is incommensurate with L_0, either kinetic or

Received: April 21, 2011
Revised: May 25, 2011
Published: July 14, 2011

ACS Publications © 2011 American Chemical Society

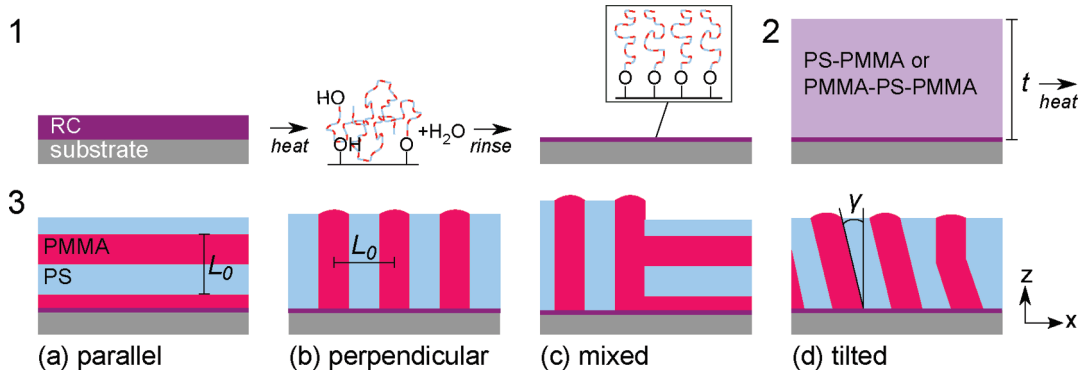

Figure 1. Overview of sample preparation and types of lamellar structures that are detected in experiments. (1) Thin film of random copolymer (RC) is cast on an ultraclean silicon substrate. Polymer is grafted to the substrate, and ungrafted polymer is removed to reveal the "neutral" polymer brush. (2) Thin film of PS-PMMA or PMMA-PS-PMMA copolymer (thickness t) is cast on top of the brush. (3) Heating above the glass transition promotes ordering of the lamellar domains. Possible outcomes are as follows: (a) parallel domain orientation, which is illustrated for asymmetric boundary conditions; (b) perfect perpendicular orientation; (c) mixed parallel and perpendicular orientations; (d) perpendicular phase with "tilt" defects, i.e., misoriented domains.

thermodynamic barriers may prevent the formation of surface relief structures, favoring perpendicular orientations to relieve entropic frustration.[10,32,34−36]

Recently, it was demonstrated that copolymer architecture can dramatically affect the free energy landscape in thin films.[37,38] Specifically, in thin films of ABA triblock copolymers, perpendicular domain orientations are stable at the air interface when the B midblock has a slightly lower surface energy than the A end blocks.[37] The effects of architecture on domain orientation were originally discussed by de Jeu et al.,[39] where it was proposed that a B-rich wetting layer would form at the air interface if the entropic penalty for "looping" was less than the surface energy gain for perpendicular domains. This description is consistent with experimental observations and self-consistent field theory (SCFT) calculations.[37] Matsen recently clarified the effects of copolymer architecture on surface energetics by noting that chain ends have a broader distribution at the free surface, so the stability of perpendicular domains largely results from increased end-segment configurational entropy.[38]

In our present work, we compare domain orientations in thin films of lamellar PS-*b*-PMMA and PMMA-*b*-PS-*b*-PMMA diblock and triblock copolymers, respectively. The melt surface energy of PS homopolymer is slightly lower than that of PMMA,[11,12] but we expect that end-segment entropy will mitigate the enthalpic preference for PS at the free surface and drive a perpendicular domain orientation. All diblock and triblock films are prepared on neutral (or near-neutral) substrates, so energetics at the air interface will largely control domain orientations through the film thickness. Film structure is characterized through optical microscopy, atomic force microscopy, and grazing-incidence small-angle X-ray scattering. For diblock copolymers, we find that domain orientations are highly sensitive to substrate surface chemistry, consistent with numerous other reports.[28,29,31−33] Perpendicular domains are reliably obtained on neutral substrates when film thickness is highly incommensurate with asymmetric boundary conditions and/or annealing temperature is elevated (≥220 °C). For triblock copolymers, we find perpendicular domain orientations in all film thicknesses considered. In addition to the expanded thickness window, we find that domain orientations in triblock films are insensitive to processing conditions (temperature, time, and variations in substrate surface chemistry), offering greater processing flexibility when compared with the diblock architecture. However, tilted domains are detected in the interior of all diblock and triblock copolymer films. The scattering data suggest that tilt defects are kinetically trapped, and their density could be minimized by reducing the copolymer molecular weight.

RESULTS AND DISCUSSION

Variables. Thin films of AB (PS-*b*-PMMA) diblock and ABA (PMMA-*b*-PS-*b*-PMMA) triblock copolymers are prepared on "neutral" polymer brushes as described in the Experimental Procedures section and illustrated in Figure 1. Film thickness, annealing temperature, annealing time, and brush quality are systematically varied to evaluate the effects of sample preparation on lamellar domain orientations. Brush quality is evaluated by measurements of the static water contact angle on freshly prepared substrates, where contact angles >80° are characteristic of a good-quality brush. More details are provided in the Experimental Procedures.

Microscopy. The surfaces of AB and ABA films are characterized with bright-field optical microscopy (OM) and atomic force microscopy (AFM). OM detects surface relief structures that are associated with parallel domain orientations, such as islands and holes, while AFM directly resolves the domain orientations at the air interface. Representative micrographs for ABA and AB films are included in Figure 2 and Figure 3, respectively, where samples were annealed on good-quality neutral brushes at 200 °C for 2 days. Significantly, ABA triblock copolymer domains are perpendicular to the air interface for all thicknesses considered: Optical micrographs reveal flat surfaces, and AFM confirms the presence of perpendicular domains. However, the structures in AB diblock copolymer films are more complex. Domains are perpendicular to the air interface when thickness t is nearly commensurate with the equilibrium copolymer periodicity L_0, i.e., $t/L_0 \leq 1$. When diblock film thicknesses are increased, the optical micrographs reveal surface modulations with an approximate wavelength of 1 μm, and AFM measurements demonstrate that these modulations correspond with mixed parallel and perpendicular domain orientations at the air interface. Parallel domain orientations are dominant in the thickest films, although perpendicular domains are often detected in regions of the film that have a slightly different thickness (for example, the dark

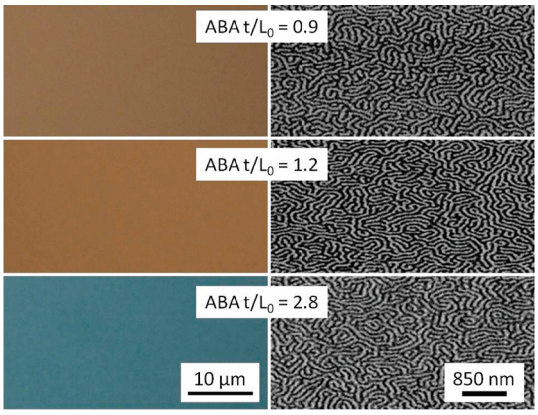

Figure 2. Bright-field optical micrographs and atomic force microscopy phase images of ABA film surfaces. All films were prepared on high-quality neutral brushes (contact angle of 83°) and annealed for 2 days at 200 °C. ABA lamellae are perpendicular to the air interface in all film thicknesses considered.

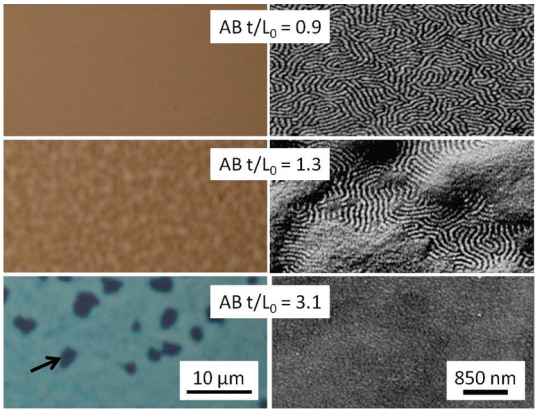

Figure 3. Bright-field optical micrographs and atomic force microscopy phase images of AB film surfaces. All films were prepared on high-quality neutral brushes (contact angle of 83°) and annealed for 2 days at 200 °C. AB domains are perpendicular to the air interface when $t/L_0 \leq 1$. Mixed parallel and perpendicular orientations are detected when $1 < t/L_0 \leq 2$, and further increases in film thickness favor a parallel orientation.

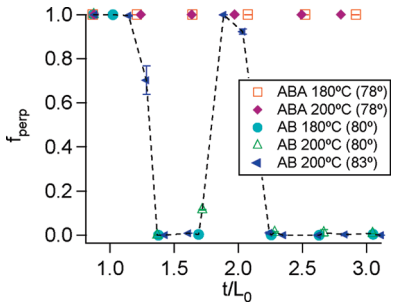

Figure 4. Fraction of perpendicular lamellae calculated from AFM images as a function of normalized film thickness. Data for "equilibrium" annealing (more than 1 day under low vacuum). Legend explains the copolymer architecture, annealing temperature, and contact angle of water on the "neutral" polymer brush. For ABA triblock copolymers, the lamellae are oriented perpendicular to the air interface in all film thicknesses studied. However, for AB diblock copolymer thin films, the lamellae are largely parallel to the surfaces when film thickness exceeds L_0. The dashed line is a guide to the eye for AB copolymer behavior.

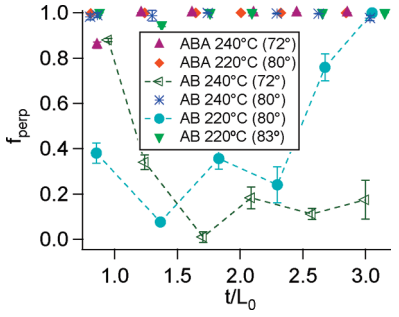

Figure 5. Fraction of perpendicular lamellae calculated from AFM images as a function of normalized film thickness. Data for "non-equilibrium" annealing (10 min in air). Legend explains the copolymer architecture, annealing temperature, and contact angle of water on the "neutral" polymer brush. For ABA triblock copolymers on brushes of moderate to good quality, the lamellae are oriented perpendicular to the air interface in all film thicknesses studied. When the brush quality is poor (72°), the thinnest ABA films show a mixture of parallel and perpendicular ordering. Thin films of AB diblock copolymers are far more sensitive to brush quality and annealing temperature.

spots marked by the arrow in Figure 3). Such mixed orientations are common when PS−PMMA films are cast on nearly neutral substrates, indicating that energetics at the substrate and free surface are not perfectly balanced.[28,29,31,32,40,41]

The micrographs in Figures 2 and 3 illustrate the types of surface structures that are detected in these experiments, but these data correspond to a specific processing scheme. Figure 4 and Figure 5 summarize the effects of each independent variable on domain orientations at the air interface for both long ("equilibrium") and short ("non-equilibrium") annealing processes, respectively. The quality of "neutral" brushes is indicated by the contact angle of water, where the maximum value of 83° corresponds with the highest grafting density. The parameter f_{perp} denotes the area fraction of each surface that contains perpendicular domains, and these data are based on analysis of AFM images as described in the Experimental Procedures.

Figure 4 summarizes f_{perp} as a function of copolymer architecture, film thickness, quality of the neutral brush (contact angle), and annealing temperature. All samples were annealed for a minimum of 1 day under low vacuum. The prolonged annealing time was selected to bring these structures toward their equilibrium conformations, and no degradation was detected at these moderate annealing temperatures. We find that ABA domains are perpendicular to the air interface ($f_{perp} = 1$) for all processing conditions and film thicknesses considered, indicating that surface energetics are controlling the triblock domain orientations. However, the AB domain orientations vary with film thickness: Lamellae are parallel to the air interface when $t = (n + 1/2)L_0$, a signature of asymmetric wetting at the interfaces.[9,10] Since the air interface is PS selective,[11,42] these data suggest that PMMA end-blocks are penetrating the neutral brush and interacting with the silicon substrate,[40] i.e., the substrate is slightly selective toward PMMA. Diblock lamellae are perpendicular to the air interface when film thickness is $t \simeq nL_0$, or highly incommensurate with asymmetric boundary conditions. Incommensurability will typically drive the formation of islands or holes.[9,12,43] In this system, either kinetic or thermodynamic barriers prevent the formation of

dx.doi.org/10.1021/ma2009222 |*Macromolecules* 2011, 44, 6121–6127

surface relief structures, favoring perpendicular orientations to relieve entropic frustration.[10,32,34−36]

Figure 5 summarizes f_{perp} as a function of copolymer architecture, film thickness, quality of the neutral brush, and annealing temperature. All samples were annealed for 10 min in air. The short annealing times are relevant to applications in manufacturing. Much like the "equilibrium" process, ABA domains are oriented perpendicular to the air interface for nearly all processing conditions considered. An exception is an ultrathin film ($t/L_0 \leq 1$) prepared on a poor-quality neutral brush, where mixed orientations are detected at the air interface. In this case, the substrate is slightly selective toward PMMA, so competition between the ordering preferred at each interface is likely responsible for the mixed orientations. AB domain orientations are more complex and depend on temperature, thickness, and brush quality. When brush quality is poor (<80°), mixed parallel and perpendicular domain orientations are detected, where the former is dominant. However, perpendicular domain orientations are detected at the air interface when brush quality is improved (≥80°) and annealing temperatures are elevated (≥220 °C). These data suggest that the surface energies of PS and PMMA are nearly equal at elevated temperatures, consistent with prior reports,[31,40] and demonstrate the well-documented sensitivity to substrate surface chemistry.[3]

Optical microscopy and AFM offer simple routes to characterize domain orientations at the air interface: Optical microscopy can quickly screen for thickness modulations that are characteristic of mixed domain orientations, while AFM measurements can discern the relative quantities of parallel and perpendicular domains at the free surface. However, it is important to note that surface microscopies cannot distiguish between perpendicular and "tilted" domain orientations (see illustration in Figure 1). Furthermore, these microscopies cannot resolve the structures at the polymer−substrate interface. We therefore evaluate AB and ABA domain orientations through the film thickness with grazing-incidence small-angle X-ray scattering (GISAXS).[44−46] In the subsequent section, we refer to a "perpendicular phase" that contains a distribution of domain orientations, and we quantify the range of tilt angles for misoriented domains through analysis of GISAXS patterns.

GISAXS Analysis. To evaluate the buried domain structure of AB and ABA thin films, GISAXS data were collected from four types of samples: AB films annealed for 2 days at 200 °C, AB films annealed for 10 min at 240 °C, ABA films annealed for 2 days at 200 °C, and ABA films annealed for 10 min at 240 °C. The brush quality was good for all samples (contact angle >80°), so we expect that surface energetics will largely control the domain orienations through the film thickness. Details regarding beamline configuration and data storage are provided in the Experimental Procedures. It is important to note that incident angle (α_i) was varied near the critical angle of the film ($\alpha_c \approx 0.17°$) to control the X-ray penetration depth. It is difficult to accurately calculate a penetration depth from the incident angle, but the top ∼10 nm is sampled when $\alpha_i < \alpha_c$, while the full film thickness is sampled when $\alpha_i > \alpha_c$.[45] All GISAXS results are consistent with the findings from microscopy: Perpendicular diblock domains were detected with GISAXS when $t \simeq nL_0$ and/or annealing temperatures were elevated, while perpendicular triblock domains were detected for all processing conditions considered. Diblock films that showed "mixed" parallel and perpendicular orientations are not discussed in this section.

When the full film thickness is sampled ($\alpha_i > \alpha_c$), nearly all diblock and triblock copolymer films show partial Debye−Scherrer (powder) rings.[47] Such features are consistent with a distribution of tilted domain orientations in the interior of these films. The range of tilt angles is denoted by $\pm\gamma$ as illustrated in Figure 1, where $\gamma = 0$ denotes a perfect perpendicular orientation. The parameter γ is determined for each data set by comparing simulated and experimental Debye−Scherrer rings in $(2\theta, \alpha)$ space. Partial rings are simulated with a straightforward procedure: First, the scattering vector for lamellae tilted through an angle $\pm\gamma$ is defined as $\vec{q}_r = \vec{q} \cdot R$, where $\vec{q} = \{q_{xy}, q_z\} = \{2\pi/L_0, 0\}$ is the scattering vector for perpendicular lamellae and R is a two-dimensional rotation matrix. Second, the contours for partial Debye−Scherrer rings in $(2\theta, \alpha)$ space are calculated from eqs 1-2:[44−46]

$$\alpha = arcsin\sqrt{\left(\frac{q_{z,r}}{k}\right)^2 + sin^2\,\alpha_i \pm 2\frac{q_{z,r}}{k}\sqrt{n^2 - 1 + sin^2\,\alpha_i}} \quad (1)$$

$$2\theta = arccos\left(\frac{cos^2\,\alpha + cos^2\,\alpha_i - (q_{xy,r}/k)^2}{2\,cos\,\alpha\,cos\,\alpha_i}\right) \quad (2)$$

Note that parameters n and α_i are the refractive index of PS−PMMA and GISAXS incident angle, respectively, while $k = 2\pi/\lambda$. Tilt range $\pm\gamma$ was refined for each sample by comparing the predicted contour of partial Debye−Scherrer rings with experimental data for $\alpha_i > \alpha_c$; simulated contours are truncated where the intensity falls to 10% of the signal from perfectly perpendicular domains ($\gamma = 0$). This procedure is illustrated in Figure 6 for triblock and diblock films with thickness $t/L_0 \simeq 3$, where calculated contours are superimposed over experimental GISAXS data for a range of incident angles. The tilt ranges calculated with this procedure are summarized in Figure 7 as a function of copolymer architecture, film thickness, and thermal history. Both diblock and triblock copolymers (ABA) form lamellae that range in orientation from perpendicular to tilted, where the maximum tilt angle γ roughly increases with film thickness. A maximum tilt angle of $(45 \pm 10)°$ is detected in films that are approximately three times thicker than the equilibrium periodicity ($t \simeq 3L_0$).

When we restrict the GISAXS measurements to the top ∼10 nm of the film ($\alpha_i < \alpha_c$), we find evidence that diblock and triblock domain orientations are different at the free surface. In diblock films, domains are perfectly perpendicular at the air interface ($\gamma = 0 \pm 10°$). In triblock films, the first-order diffraction peak is asymmetric in all samples, and the peak shape is consistent with the predicted profile for tilted domains. Such characteristics are observed in Figure 6a when $\alpha_i = 0.11°$. However, it is very difficult to distinguish between tilted domains and poorly ordered perpendicular domains when $\alpha_i < \alpha_c$, so it is unclear if the tilt really persists at the near-surface region.

Tilted lamellae have been predicted and observed in AB copolymers assembled on incommensurate chemical templates.[48−52] In such systems, the chemical patterns have a strong affinity for a specific domain. When the pitch of chemical patterns is larger than L_0, the domains must either stretch to match the template or tilt to minimize the stretching penalty. In the present system, there is no periodic potential at the surfaces that could induce such frustration. We speculate that misoriented domains are kinetically trapped: The

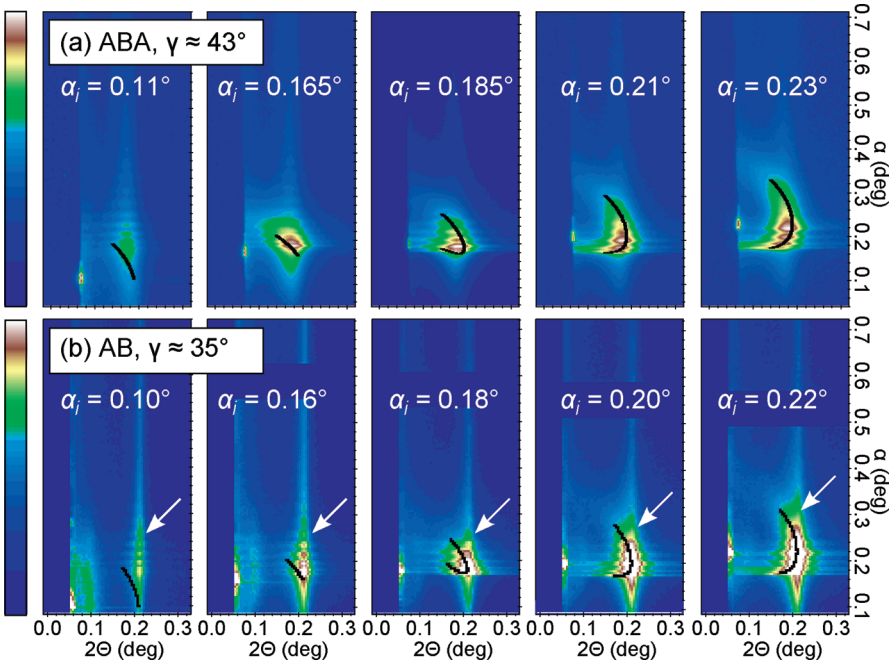

Figure 6. GISAXS data for (a) triblock and (b) diblock copolymer thin films ($t/L_0 = 2.9$) annealed at 240 °C for 10 min. Incident angle (α_i) is varied near the critical angle (0.17°) to produce controlled penetration depths. Contours for partial Debye−Scherrer rings are superimposed over experimental data (solid black lines). The ranges of lamellar tilt angles are $\gamma = (43 \pm 10)°$ and $\gamma = (35 \pm 10)°$ for triblock and diblock morphologies, respectively. Note that AB domains are not tilted near the air interface (contours are included as a guide to the eye). The weak "streaks" extending along the α-axis at $2\theta \approx 0.2°$ are associated with the surface topography (PMMA protrusions illustrated in Figure 1), and these features are discussed in the Appendix.

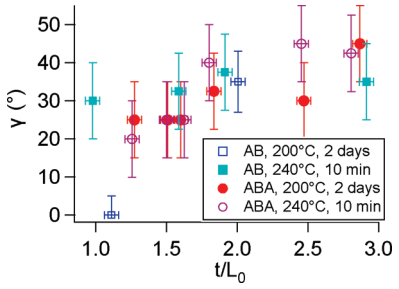

Figure 7. Summary of maximum lamellar tilt angles ($\pm\gamma$) for all samples measured with GISAXS. Thin films of diblock (AB) and triblock (ABA) copolymers almost always contain some tilted lamellae, and the degree of misorientation increases with film thickness.

molecular weights of our AB and ABA copolymers are approximately 100 kDa and 200 kDa, respectively, so entanglements and slow diffusion could limit the rate of ordering.[53,54] Furthermore, it is well-known that the energetic cost for bending lamellar domains is very small, as evidenced by "finger-print" patterns in thin films,[25,52] curved domains and "T-junctions" on epitaxial templates,[55−57] and mixed domain orientations in thick copolymer films.[41,58,59] Considering our high molecular weights and the small energetic penalty for lamellar curvature, it is unlikely that further annealing would change the domain orientations. This is confirmed with in situ GISAXS measurements, where additional annealing for 1 day at 235 °C produces no detectable change in domain orientations.

Our GISAXS data suggest that reducing the molecular weights could improve the quality of AB and ABA thin films: Diblocks have a narrower line shape than triblocks, indicating they possess a higher degree of lateral order. Diblocks are also characterized by

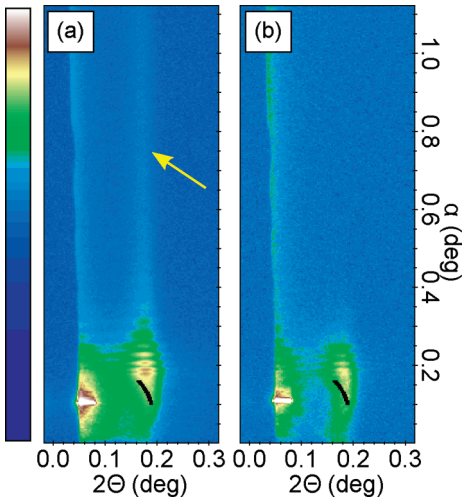

Figure 8. In situ GISAXS from ABA triblock copolymer ($t/L_0 \simeq 2.5$). Data were collected at an incident angle of $\alpha_i = 0.1°$, i.e., below the critical angle. (a) Sample prior to heating. (b) Sample heated to 85 °C. Surface topography vanishes upon heating, and does not reappear when cooled to room temperature (under vacuum).

a "split" first-order diffraction peak when $\alpha_i > \alpha_c$, where these two peaks are associated with a "perfect" perpendicular phase and tilted domains, respectively. The diffraction peak associated with the "perfectly" oriented domains is noted by the arrow in Figure 6b. In contrast, the higher molecular weight triblocks assemble into an imperfect perpendicular phase, meaning the film is characterized by a distribution of tilted domains with poor lateral ordering.

dx.doi.org/10.1021/ma2009222 |*Macromolecules* 2011, 44, 6121–6127

CONCLUSIONS

Domain orientations in thin films of lamellar poly(styrene-*b*-methyl methacrylate) (AB) and poly(methyl methacrylate-*b*-styrene-*b*-methyl methacrylate) (ABA) copolymers were evaluated as a function of film thickness, annealing temperature, and annealing time. The objective was to identify conditions that offer a perpendicular domain orientation in thin films, emphasizing films that are thicker than the equilibrium domain periodicity L_0. Substrates were energetically "neutral" (or nearly neutral) with respect to the copolymer constituents, so domain orientations were largely controlled by surface energetics. For AB diblocks, the perpendicular orientation was reliably obtained for a broad range of film thickness when annealing temperatures were elevated (>220 °C) and the substrates had few imperfections. Reduced annealing temperatures and/or damaged substrates produce a mixture of parallel and perpendicular domain orientations. For ABA triblocks, the perpendicular domain orientation was easily generated for a broad range of film thicknesses and processing conditions, demonstrating the entropic preference for A end blocks at the free surface. Significantly, the data demonstrate that perpendicular domains are more easily achieved with triblocks than diblocks, particular in thicker films. Such behavior is beneficial for lithographic applications that require high-aspect-ratio nanostructures (such as plasma etching).[60] However, the perpendicular phase in both diblocks and triblocks contains a high density of kinetically trapped defects such as "tilted" domains. Longer annealing times did not reduce the defect density, but the data suggest that reducing the molecular weight of these copolymers will improve both the domain orientation and lateral ordering.

EXPERIMENTAL PROCEDURES

Materials. All polymers were purchased from Polymer Source and used as received. "Neutral" polymer brushes are prepared from a hydroxyl-terminated poly(styrene-*co*-methyl methacrylate) random copolymer that is 59 mol % styrene with M_n = 8.9 kg/mol and PDI = 1.47. (The styrene content is slightly higher than the reported "optimal" composition for lamellar copolymers,[28] but we find that substrates treated with this copolymer are slightly selective toward methyl methacrylate.) The AB diblock copolymer is poly(styrene-*b*-methyl methacrylate) (PS−PMMA), with M_n = 100 kg/mol, PDI = 1.12, and 50 mol % styrene. The ABA triblock is poly(methyl methacrylate-*b*-styrene-*b*-methyl methacrylate) (PMMA-PS-PMMA), with M_n = 198 kg/mol, PDI = 1.15, and 50 mol % styrene. Equilibrium lamellar periodicity (L_0) for AB and ABA copolymers are 46 and 50 nm, respectively, as determined with X-ray scattering. Substrates are (100) oriented silicon wafers with minimal bow (per the manufacturer). Substrates are cleaned with Piranha solution (3:1 H_2SO_4:30% H_2O_2, *Caution! Highly Corrosive*) to destroy organic contamination and grow a thin oxide layer.

"Neutral" Substrates. Random copolymer is dissolved in toluene at a concentration of 1 wt %, and films that are approximately 30 nm thick are prepared by spin-casting on ultraclean silicon substrates. Polymer chains are grafted to the substrate by annealing under low vacuum (10 mTorr) with the following temperature profile: 80 °C for 2 h, then 160 °C for 1 day, followed by cooling to room temperature. Ungrafted polymer is extracted by agitating the samples in toluene (using a sonication bath) or soaking in a stationary toluene bath for 1 h. Samples are then dried with nitrogen. The quality (density) of the brush is assessed by measuring the contact angle of water, which is usually 72° after this process. Contact angle is increased to 80−83° by repeating all steps a second time (includes coating a new film, annealing, and rinsing); these measured contact angles match the reported values in the literature.[28] Throughout this manuscript, the different brush qualities are denoted by the contact angle of water at the surface.

AB and ABA Thin Films. Thin films of AB and ABA block copolymers are prepared on the "neutral" brushes. Polymers are dissolved in toluene at concentrations that range from 1 to 4 wt %; solutions are filtered with a 0.2 μm Teflon mesh. Films that range in thickness from 40 to 200 nm are prepared by spin-casting. Film thicknesses are measured with a JA Wollam M-2000 spectroscopic ellipsometer: Δ and Ψ are modeled with the Cauchy dispersion relation $n(\lambda) = A + B/\lambda^2$, where A, B, and film thickness are adjustable parameters for regression analysis (all positive values). Films are annealed according to two different procedures: Samples prepared via a "non-equilibrium" process are annealed in air for 10 min at 220 or 240 °C. Samples prepared by an "equilibrium" process are annealed under low vacuum (10 mTorr) for 1−2 days at either 180 or 200 °C. The segregation strength is approximately $\chi N \simeq 45$ at temperatures in the range of 180 to 240 °C.[61]

Microscopy. The nanoscale and microscale structure of film surfaces are characterized with atomic force microscopy (AFM) and bright-field optical microscopy, respectively. AFM micrographs were collected with a MultiMode 3 (Veeco) in tapping mode using silicon probes with a spring constant of approximately 40 N/m. Typical parameters for data acquisition are 1.7 Hz scan frequency, 5 μm × 5 μm scan area, and 512 × 512 image resolution. Each sample is measured from at least five randomly selected regions, and the fraction of perpendicular lamellae per micrograph is calculated with an algorithm implemented in ImageJ. Optical micrographs can detect variations in sample thickness over microscale areas that are associated with either parallel or mixed parallel/perpendicular lamellar orientations.

Grazing-Incidence Small Angle X-ray Scattering (GISAXS). GISAXS experiments (see Figure 8) were conducted at beamline 8-ID-E at the Advanced Photon Source of Argonne National Laboratory. Samples were placed in a vacuum chamber and illuminated with 7.35 keV radiation at incident angles in the range of 0.1−0.24°; the off-specular scattering was recorded with one of the following configurations: A MAR 165 ccd-based detector (pixel size = 79 μm) positioned 2019 mm from the sample, or a Pilatus 1MF pixel array detector (pixel size = 172 μm) positioned 2175 mm from the sample. Acquisition times were approximately 10 s per frame. Each data set is stored as a 2048 × 2048 16-bit tiff image (MAR) or as a 981 × 1043 32-bit tiff image (Pilatus, with 20-bit dynamic range). Note that X-ray penetration depth varies from approximately 10 nm up to the full film thickness as incident angle is varied near the critical angle of the film (ca. 0.17°). All data are displayed as intensity maps $I(2\theta, \alpha)$, where 2θ and α denote in-plane and out-of-plane diffraction angles, respectively.

APPENDIX

A Comment on Surface Topography. Both diblock and triblock thin films exhibit a very weak peak centered near $2\theta \sim 0.2°$ that extends along the entire α-axis. This feature is associated with the surface topography that is qualitatively illustrated in Figure 1.[45,62] We speculate that PMMA is absorbing moisture from the ambient environment, which swells the PMMA domains and generates protrusions at the free interface. (It is well-documented that PMMA domains are "taller" in AFM measurements; see, for example, a paper from Thurn-Albrecht et al.[63]) This hypothesis is supported by in-situ GISAXS measurements, where we observe that surface scattering disappears upon heating at moderate temperature (85°C). Surface scattering does not reappear when samples are cooled under vacuum. Representative data are included in Figure 8 for a triblock copolymer film.

AUTHOR INFORMATION

Author Contributions

[†]Equally contributing authors.

■ ACKNOWLEDGMENT

The authors acknowledge financial support by the National Science Foundation under Grant No. EEC/ECCS-0927147 and UH GEAR program under Grant No. 98520. T.V. thanks the UH Summer Undergraduate Research Fellowship, Provost's Undergraduate Research Scholarship, and the ChBE Undergraduate Senior Thesis Award for financial support. Use of the Advanced Photon Source was supported by the U.S. Department of Energy, Office of Science, Office of Basic Energy Sciences, under Contract No. DE-AC02-06CH11357. We thank Joseph Strzalka and Jin Wang for assistance with GISAXS measurements, and we thank Peter Vekilov for use of the MultiMode AFM.

■ REFERENCES

(1) Segalman, R. *Mater. Sci. Eng. R-Rep.* **2005**, *48*, 191–226.
(2) Black, C.; Ruiz, R.; Breyta, G.; Cheng, J.; Colburn, M.; Guarini, K.; Kim, H.-C.; Zhang, Y. *IBM J. Res. Dev.* **2007**, *51*, 605–633.
(3) Bang, J.; Jeong, U.; Ryu, D.; Russell, T.; Hawker, C. *Adv. Mater.* **2009**, *21*, 4769–4792.
(4) Bates, F.; Fredrickson, G. *Annu. Rev. Phys. Chem.* **1990**, *41*, 525–557.
(5) Segalman, R.; Yokoyama, H.; Kramer, E. *Adv. Mater.* **2001**, *13*, 1152–1155.
(6) Cheng, J.; Ross, C.; Thomas, E.; Smith, H.; Vancso, G. *Appl. Phys. Lett.* **2002**, *81*, 3657–3659.
(7) Kim, S.; Solak, H.; Stoykovich, M.; Ferrier, N.; de Pablo, J.; Nealey, P. *Nature* **2003**, *424*, 411–414.
(8) Stoykovich, M.; Muller, M.; Kim, S.; Solak, H.; Edwards, E.; de Pablo, J.; Nealey, P. *Science* **2005**, *308*, 1442–1446.
(9) Fasolka, M.; Mayes, A. *Annu. Rev. Mater. Res.* **2001**, *31*, 323–355.
(10) Matsen, M. *J. Chem. Phys.* **1997**, *106*, 7781–7791.
(11) Coulon, G.; Russell, T.; Deline, V.; Green, P. *Macromolecules* **1989**, *22*, 2581–2589.
(12) Coulon, G.; Collin, B.; Ausserre, D.; Chatenay, D.; Russell, T. *J. Phys. (Paris)* **1990**, *51*, 2801–2811.
(13) Anastasiadis, S.; Russell, T.; Satija, S.; Majkrzak, C. *Phys. Rev. Lett.* **1989**, *62*, 1852–1855.
(14) Anastasiadis, S.; Russell, T.; Satija, S.; Majkrzak, C. *J. Chem. Phys.* **1990**, *92*, 5677–5691.
(15) Mayes, A.; Russell, T.; Bassereau, P.; Baker, S.; Smith, G. *Macromolecules* **1994**, *27*, 749–755.
(16) Morkved, T.; Lu, M.; Urbas, A.; Ehrichs, E.; Jaeger, H.; Mansky, P.; Russell, T. *Science* **1996**, *273*, 931–933.
(17) Sivaniah, E.; Hayashi, Y.; Iino, M.; Hashimoto, T.; Fukunaga, K. *Macromolecules* **2003**, *36*, 5894–5896.
(18) Yager, K.; Berry, B.; Page, K.; Patton, D.; Karim, A.; Amis, E. *Soft Matter* **2009**, *5*, 622–628.
(19) Kim, G.; Libera, M. *Macromolecules* **1998**, *31*, 2569–2577.
(20) Kim, S.; Misner, M.; Xu, T.; Kimura, M.; Russell, T. *Adv. Mater.* **2004**, *16*, 226–229.
(21) Huang, E.; Russell, T.; Harrison, C.; Chaikin, P.; Register, R.; Hawker, C.; Mays, J. *Macromolecules* **1998**, *31*, 7641–7650.
(22) Lin, Y.; Boker, A.; He, J.; Sill, K.; Xiang, H.; Abetz, C.; Li, X.; Wang, J.; Emrick, T.; Long, S.; Wang, Q.; Balazs, A.; Russell, T. *Nature* **2005**, *434*, 55–59.
(23) Son, J.; Bulliard, X.; Kang, H.; Nealey, P.; Char, K. *Adv. Mater.* **2008**, *20*, 3643–3646.
(24) Jeong, U.; Ryu, D.; Kho, D.; Kim, J.; Goldbach, J.; Kim, D.; Russell, T. *Adv. Mater.* **2004**, *16*, 533–536.
(25) Mansky, P.; Liu, Y.; Huang, E.; Russell, T.; Hawker, C. *Science* **1997**, *275*, 1458–1460.
(26) Mansky, P.; Russell, T.; Hawker, C.; Pitsikalis, M.; Mays, J. *Macromolecules* **1997**, *30*, 6810–6813.
(27) Ryu, D.; Shin, K.; Drockenmuller, E.; Hawker, C.; Russell, T. *Science* **2005**, *308*, 236–239.
(28) Ham, S.; Shin, C.; Kim, E.; Ryu, D.; Jeong, U.; Russell, T.; Hawker, C. *Macromolecules* **2008**, *41*, 6431–6437.
(29) Han, E.; Stuen, K.; La, Y.-H.; Nealey, P.; Gopalan, P. *Macromolecules* **2008**, *41*, 9090–9097.
(30) Ji, S.; Liu, C.-C.; Son, J.; Gotrik, K.; Craig, G.; Gopalan, P.; Himpsel, F.; Char, K.; Nealey, P. *Macromolecules* **2008**, *41*, 9098–9103.
(31) Han, E.; Stuen, K.; Leolukman, M.; Liu, C.-C.; Nealey, P.; Gopalan, P. *Macromolecules* **2009**, *42*, 4896–4901.
(32) Suh, H.; Kang, H.; Liu, C.-C.; Nealey, P.; Char, K. *Macromolecules* **2010**, *43*, 461–466.
(33) Bates, C.; Strahan, J.; Santos, L.; Mueller, B.; Bamgbade, B.; Lee, J.; Katzenstein, J.; Ellison, C.; Willson, C. *Langmuir* **2011**, *27*, 2000–2006.
(34) Russell, T.; Menelle, A.; Anastasiadis, S.; Satija, S.; Majkrzak, C. *Macromolecules* **1991**, *24*, 6263–6269.
(35) Turner, M. *Phys. Rev. Lett.* **1992**, *69*, 1788–1791.
(36) Koneripalli, N.; Bates, F.; Fredrickson, G. *Phys. Rev. Lett.* **1998**, *81*, 1861–1864.
(37) Khanna, V.; Cochran, E.; Hexemer, A.; Stein, G.; Fredrickson, G.; Kramer, E.; Li, X.; Wang, J.; Hahn, S. *Macromolecules* **2006**, *39*, 9346–9356.
(38) Matsen, M. *Macromolecules* **2010**, *43*, 1671–1674.
(39) De Jeu, W.; Lambooy, P.; Hamley, I.; Vaknin, D.; Pedersen, J.; Kjaer, K.; Seyger, R.; Vanhutten, P.; Hadziioannou, G. *J. Phys. II* **1993**, *3*, 139–146.
(40) Mansky, P.; Russell, T.; Hawker, C.; Mays, J.; Cook, D.; Satija, S. *Phys. Rev. Lett.* **1997**, *79*, 237–240.
(41) Huang, E.; Mansky, P.; Russell, T.; Harrison, C.; Chaikin, P.; Register, R.; Hawker, C.; Mays, J. *Macromolecules* **2000**, *33*, 80–88.
(42) Russell, T.; Coulon, G.; Deline, V.; Miller, D. *Macromolecules* **1989**, *22*, 4600–4606.
(43) Green, P.; Limary, R. *Adv. Colloid Interface Sci.* **2001**, *94*, 53–81.
(44) Lee, B.; Park, I.; Yoon, J.; Park, S.; Kim, J.; Kim, K.; Chang, T.; Ree, M. *Macromolecules* **2005**, *38*, 4311–4323.
(45) Stein, G.; Kramer, E.; Li, X.; Wang, J. *Macromolecules* **2007**, *40*, 2453–2460.
(46) Renaud, G.; Lazzari, R.; Leroy, F. *Surf. Sci. Rep.* **2009**, *64*, 255–380.
(47) Busch, P.; Rauscher, M.; Moulin, J.-F.; Mueller-Buschbaum, P. *J. Appl. Crystallogr.* **2011**, *44*, 370–379.
(48) Tsori, Y.; Andelman, D. *J. Chem. Phys.* **2001**, *115*, 1970–1978.
(49) Tsori, Y.; Andelman, D. *Europhys. Lett.* **2001**, *53*, 722–728.
(50) Tsori, Y.; Andelman, D. *Interface Sci.* **2003**, *11*, 259–268.
(51) Wang, Q. *Macromol. Theory Simul.* **2005**, *14*, 96–108.
(52) Kim, S.; Kim, B.; Kim, K.; Koo, C.; Stoykovich, M.; Nealey, P.; Solak, H. *Macromolecules* **2006**, *39*, 5466–5470.
(53) Lodge, T.; Dalvi, M. *Phys. Rev. Lett.* **1995**, *75*, 657–660.
(54) Fredrickson, G.; Bates, F. *Annu. Rev. Mater. Sci.* **1996**, *26*, 501–550.
(55) Wilmes, G.; Durkee, D.; Balsara, N.; Liddle, J. *Macromolecules* **2006**, *39*, 2435–2437.
(56) Stoykovich, M.; Kang, H.; Daoulas, K.; Liu, G.; Liu, C.-C.; de Pablo, J.; Mueller, M.; Nealey, P. *ACS Nano* **2007**, *1*, 168–175.
(57) Chai, J.; Buriak, J. *ACS Nano* **2008**, *2*, 489–501.
(58) Xu, T.; Hawker, C.; Russell, T. *Macromolecules* **2005**, *38*, 2802–2805.
(59) Zucchi, I.; Poliani, E.; Perego, M. *Nanotechnology* 2010, *21*, Art. No. 185304
(60) Liu, C.-C.; Nealey, P.; Ting, Y.-H.; Wendt, A. *J. Vac. Sci. Technol. B* **2007**, *25*, 1963–1968.
(61) Zhao, Y.; Sivaniah, E.; Hashimoto, T. *Macromolecules* **2008**, *41*, 9948–9951.
(62) Bang, J.; Kim, B.; Stein, G.; Russell, T.; Li, X.; Wang, J.; Kramer, E.; Hawker, C. *Macromolecules* **2007**, *40*, 7019–7025.
(63) Thurn-Albrecht, T.; Steiner, R.; DeRouchey, J.; Stafford, C.; Huang, E.; Bal, M.; Tuominen, M.; Hawker, C.; Russell, T. *Adv. Mater.* **2000**, *12*, 787–791.